Western and
Central Pacific
Fisheries
Commission

SCIENTIFIC COMMITTEE
TWENTIETH REGULAR SESSION

Manila, Philippines
14 – 21 August 2024

Development of Dynamic Energy Budget model of yellowfin tuna *(Thunnus albacares)* and its potential applications using archival tagging data

WCPFC-SC20-2024/SA-IP-21

Takaaki Hasegawa, Yoshinori Aoki, Hirotaka Ijima, Kei Okamoto, Keisuke Satoh,
Joe Scutt Phillips, Daniel W. Fuller and Marko Jusup

Development of a Dynamic Energy Budget model for yellowfin tuna (*Thunnus albacares*) and its potential applications using archival tagging data

Takaaki Hasegawa[1], Yoshinori Aoki[1], Hirotaka Ijima[1], Kei Okamoto[1], Keisuke Satoh[1], Joe Scutt Phillips[2], Daniel W. Fuller[3] and Marko Jusup[1]

[1]Fisheries Research and Education Agency, Fisheries Resources Institute, Yokohama, Japan.

[2]Pacific Community, Ocean Fisheries Programme, Noumea, New Caledonia.

[3]Inter-American Tropical Tuna Commission, La Jolla, California, USA.

Abstract

The Tropical Pacific Ocean features unique oceanographic characteristics with high environmental variability on the large scale, such as the El Niño-Southern Oscillation (ENSO), affecting the distribution and biomass of tunas. Predicting population dynamics in response to environmental variability requires understanding how environmental factors influence life-history traits (growth, maturity, and reproduction). As an approach to this problem based on physiological energetics, the Dynamic Energy Budget (DEB) theory quantifies the processes by which an organism acquires and allocates energy for survival, growth, maturation, and reproduction. The DEB theory is unique in capturing the metabolic processes of an organism throughout its entire life cycle as a function of temperature and food abundance. This document reports on the development of a DEB model for yellowfin tuna (*Thunnus albacares*), covering its entire life cycle from an egg to a spawning adult and its eggs. Using a comprehensive dataset on the life-history traits of this species, we successfully estimated model parameters, uncovering the energy budget of yellowfin tuna across all life stages. We present preliminary estimates of field food consumption for archival-tagged fish, based on their growth and ambient temperature data. We discuss potential applications of this model.

Introduction

The Tropical Pacific Ocean is characterized by high environmental variability, influenced by marine currents and climatic events like the El Niño-Southern Oscillation (ENSO). These conditions can affect the distribution and abundance of marine species, with impacts on fisheries dynamics for tropical tunas (Lehodey et al. 1997). To predict tuna population dynamics in response to environmental variability, it is important to understand how environmental factors influence life-history traits such as growth, maturity, and reproduction.

Dynamic Energy Budget (DEB) theory quantifies the processes by which an organism acquires and allocates energy for survival, growth, maturation, and reproduction (Koojiman 2010). The DEB theory is unique in capturing the metabolic processes of an organism throughout its entire life cycle as a function of temperature and food abundance. Thus, the DEB model can be a useful tool to explore the physiological mechanism by which environmental factors affect growth, maturity and reproduction.

This document aims to describe the development of a DEB model for yellowfin tuna (*Thunnus albacares*). Using a comprehensive dataset on the life-history traits of this species, we estimated the model parameters, covering its entire life cycle from an egg to a spawning adult and its eggs. The model can be applied to estimate the energy intake of an individual fish as a function of its growth and ambient temperature. Using the length at release and recapture information of archival-tagged fish along with recorded ambient temperature data, we present preliminary estimates of their field food consumption. Finally, we discuss other potential applications of the model.

Materials and Methods

Model structure

Building on existing descriptions of the DEB model for tuna (Jusup et al. 2011, 2014), we focus on key concepts. The DEB model describes energy flows of a fish throughout its life cycle while accounting for environmental factors such as temperature and food abundance (Figure 1). The model tracks the energy flow among the following four state variables:

1. **Energy reserves (E)**: Amount of energy in reserve potentially available for metabolic processes.
2. **Structural volumetric length (L)**: Amount of energy accumulated into structure, which is an abstract quantity of physical length of an organism.
3. **Level of maturity (E_H)**: Amount of energy accumulated for maturation, which tracks the developmental state of an organism.
4. **Reproduction buffer (E_R)**: Amount of energy accumulated for reproduction.

The dynamics of these state variables are determined by six energy flows:

1. **Assimilation ($\dot{p}_A$)**: The rate of energy entering the reserve through assimilation.
2. **Utilization ($\dot{p}_C$)**: The rate of energy mobilized from the reserve. This flow is split according to the κ-rule: a fraction $\kappa\dot{p}_C$ serves the needs for somatic maintenance and fuels growth if there is energy available. The remaining fraction, $(1-\kappa)\dot{p}_C$, satisfies the needs for maturity maintenance and, depending on the current level of maturity, fuels maturation or reproduction if there is energy available.
3. **Somatic maintenance ($\dot{p}_S$)**: The rate of energy required to basic metabolic processes that keep the fish alive, which is differentiated between structural volume-related maintenance costs $\dot{\boldsymbol{p}}_{\boldsymbol{M}}$ and structural surface-area-related maintenance $\dot{\boldsymbol{p}}_{\boldsymbol{T}}$
4. **Growth ($\dot{p}_G$)**: The rate of energy into the structure, leading to an increase in the structural length (L). Growth stands for the change in size, which is different from maturation that stands for complexity.
5. **Maturity maintenance ($\dot{p}_J$)**: The rate of energy required to maintain the maturity state.
6. **Maturation/Reproduction ($\dot{p}_R$)**: When $E_H < E_H^p$ (before puberty), the rate of energy into the maturation, leading to an increase of complexity of structure as a preparation for the adult stage (involving extensive gene regulation switching, cell and tissue differentiation, etc.). When $E_H > E_H^p$ (adult stage), the rate of energy into the reproduction buffer, leading to production of eggs.

Equations to governing the rate of change of the state variables depending on the energy flows are given in Table 1 and Table 2. The energy flows, in turn, depend on temperature and food abundance. Temperature regulates all the energy flows through the Arrhenius relationship, which describes the effect of temperature on metabolic rates within the temperature tolerance range of an individual. The effect of temperature (T) on an energy flux is described by:

$$\dot{p}_*(T) = \dot{p}_*(T_0)\exp\left(\frac{T_A}{T_0} - \frac{T_A}{T}\right) \tag{1}$$

where T_0 is reference temperature (20 ˚C), and T_A is the Arrhenius temperature measuring how sensitive energy flows are to changes in T.

Food availability (f) influences ingestion rate, or equivalently, assimilation flow. This is a scaled quantity that takes values between 0 (starvation) and 1 (feeding ad libitum).

Relating state variables to data

The state variables in the DEB model are abstract quantities that cannot be directly measured. Therefore, for practical use, we need to convert these state variables into measurable quantities. Typically, these measurable quantities can be expressed as explicit functions of the state variables. When applying the model in conjunction with data, converting state variables into fork length, body mass, batch fecundity, and food conversion ratio (FCR) is of primary interest.

Structural length (L) of an organism in DEB is related to the organism's physical length (L_w) through the shape factor, δ_M. In isomorphic organisms, the two lengths are proportional, and δ_M is a constant. However, because tuna changes its shape as it matures, the shape factor is a function of maturity, $\delta_M \equiv \delta_M(E_H)$. The fork length is given by:

$$L_W = \frac{L}{\delta_M(E_H)} \tag{3}$$

The shape factor's functional form is such that its value increases relatively fast during early ontogeny, but becomes progressively more saturated afterwards.

Body mass of the organism is calculated by summing contributions from all relevant DEB state variables: reserve, structure, and (in adults) the reproductive buffer. The equation is:

$$W = d_V L^3 + \rho_E(E + E_R) \tag{4}$$

where d_V is the density of the structure (assumed ≈ 1.0 g·cm^{-3}) and ρ_E is the mass-energy coupler for the reserve estimated at 1.0864·10^{-4} g·J^{-1}

Batch fecundity ($\dot{F}$) is obtained by dividing the energy allocated to the reproductive buffer (E_R) by the total number of batches per year (N) and the initial energy reserve of an egg (E_0). The equation is:

$$\dot{F} = \frac{\kappa_R \times E_R}{N \times E_0} \tag{5}$$

where κ_R is the efficiency with which a mother's reserve is converted into eggs. This efficiency is typically set to a high value ($\kappa_R \approx 0.95$) because the mother's reserve and the reserve energy stored in an egg should have similar chemical compositions. Calculating the initial energy reserve (E_0) is described in the literature (Jusup et al. 2017).

Feed Conversion Ratio (FCR) is widely used as a measure of how efficiently the fish convert feed mass into the fish body mass. In general, FCR is defined as the ratio of dry weight of supplied feed to gain in wet weight of the fish.

$$\mathrm{FCR} = \frac{dW_{\mathrm{food}}}{dW} \tag{6}$$

where W_{food} represents food mass and W the body mass. Ingested food mass can be estimated from the assimilation flow

$$\frac{dW_{\mathrm{food}}}{dt} = \frac{\rho_X}{\kappa_X}\dot{p}_A \tag{7}$$

where ρ_X = 1.894·10^{-4} g·J^{-1} is the mass energy coupler for food (Jusup et al. 2014) and κ_X ($0<\kappa_X\leq 1$) is the assimilation efficiency of food into reserve. This assimilation efficiency accounts for losses associated with the inefficiency in digestive system and other assimilation overheads, such as specific dynamic action. We set κ_X=0.8 (Jusup et al. 2014). By substituting Equation 4 and Equation 7 into Equation 6, we obtain the final expression for FCR:

$$\mathrm{FCR} = \frac{\rho_X}{\kappa_X}\left[\frac{d_V \dot{p}_G}{[E_G]\dot{p}_A} + \rho_E\left(1 - \frac{\dot{p}_C}{\dot{p}_A} + \frac{\dot{p}_R}{\dot{p}_A}\right)\right]^{-1} \tag{8}$$

Data and parameter estimation

Developing a full lifecycle DEB model for yellowfin tuna requires a comprehensive life-history dataset covering all life stages. Because the model accounts for temperature and food abundance, data collected under known environmental conditions are preferable. Long-term captive studies on yellowfin tuna have been conducted by the Achotines Laboratory in Panama, run by the Inter-American Tropical Tuna Commission (Margulies et al. 2016). We primarily relied on datasets from these studies for model development, supplemented by data from other studies on wild fish in the Eastern Pacific Ocean (EPO, Table 4, Table 5). To determine the values of basic DEB and other parameters that produce the best fit of model predictions to data, we used the Nelder-Mead numerical optimization method available in the *DEBtool* software package (Kooijman et al. 2008).

Model performance

We assessed the model performance using a goodness-of-fit (GOF) measure (Jusup et al. 2011) based on the mean relative error (MRE). This was followed by a qualitative assessment of the model's success in simulating the specifics of each life stage. Intuitively, the MRE represents a "distance" between the observed data and the model estimates. More formally, let $d_{i,j}$ be the i_{th} dataset comprising n_i data points, and $e_{i,j}$ a set of the corresponding model estimates. Then the i_{th} weighted relative error is given by:

$$\mathrm{RE}_i = \sum_{j=1}^{n_i} \frac{w_{ij}}{w_i}\left|\frac{e_{ij} - d_{ij}}{d_i}\right| \tag{9}$$

where $w_{i,j}$ are the weight coefficients, $w_i = \sum_j w_{ij}$, and $d_i = \sum_j \frac{d_{ij}}{n_i}$. Furthermore, let *N* be a total number of datasets. We then have

$$\mathrm{MRE} = \frac{1}{N}\sum_{i=1}^{N} \mathrm{RE}_i$$

Because $\mathrm{MRE} = 0$ when estimates match data perfectly, we defined our GOF measure as $\mathrm{GOF} = 100 \times (1 - \mathrm{MRE})$, with a maximum score of 100 for a perfect fit.

Estimating food consumption for archival tagged fish

As described above, the DEB model predicts growth as a function of temperature and food abundance. By having information about the growth and ambient temperature for individual fish over a certain period, we can estimate energy intake by the fish during that time. Archival tags are useful in this sense because they can continuously record ambient temperature for individual fish, and growth data can be obtained when both the length at release and the length at recapture are available. We used archival tagging data collected in the Western and Central Pacific Ocean (WCPO) by the Pacific Tuna Tagging Program (PTTP) and data collected in the Eastern Pacific Ocean (EPO) by the IATTC tagging program to estimate their field food consumption. An overview of the data is provided in Table 6.

To estimate field food consumption, we used the following symbolic equation:

$$L_{t+\Delta_\mathrm{t}} = F\big(\, L_t, \mathit{\Delta}_t, T_\mathrm{avg} \mid f \,\big)$$

where F stands for the generalized growth function given by the DEB model, $L_{t+\Delta_\mathrm{t}}$ is the length at recapture, L_t is the length at release, $\mathit{\Delta}_t$ is the elapsed days between release and recapture, T_avg is the 7-day moving average of ambient temperature recorded by the archival tag, f is the scaled food abundance and the quantity to estimate. We used this equation to find the optimal value of f that minimizes the difference between the predicted and actual length at recapture. This optimization was achieved using the *fminsearch* function in MATLAB. Then we converted the f to the actual food mass (g) with the following equation:

$$W_\mathrm{food} \;=\; \frac{f \times \rho_X \times M_1 \times p_{Am} \times (L\; \times L_m)^2}{\kappa_X}.$$

Comparing daily ration between areas

With the estimated food consumption, we can calculate daily ration of fish (percentage of daily food consumption divided by fish weight) using the following equation:

$$\text{Daily Ration (\%)} = \frac{W_\mathrm{food}}{W} \times 100$$

To compare the daily ration between the WCPO and the EPO, and determine if there is a significant difference these areas, we performed a statistical analysis that corrects for fish size and ambient temperature. First, we extracted the daily ration, length, and temperature data at three points: at release, at recapture, and as averages over the recorded period for each individual fish. We then used these extracted data points for the analysis.

We used a linear mixed-effects model (Bates et al. 2014) to evaluate the effect of area while accounting for length and temperature as fixed effects, and individual variability as a random effect. The model was defined as follows:

$$\text{Daily Ration} \;=\; \beta_0 + \beta_1 \cdot \text{Area} + \beta_2 \cdot \text{Length} + \beta_3 \cdot \text{Temperature} + \text{ID}$$

where β_0 is the intercept, β_1, β_2, and β_3 are the coefficients for the fixed effects, and $ID \sim N(0, \sigma^2)$ represents the individual effect, assumed to follow a normal distribution with mean zero and variance σ^2.

To assess the effect of area, we compared the full model, which includes the area as a fixed effect, with a model that excludes the area effect. The significance of the area effect was determined based on the resulting p-value from the likelihood ratio test.

To evaluate the goodness of fit of our model, we calculated the coefficients of determination R^2, which is a measure of the proportion of variability in the dependent variable that is explained by the independent variables in the model. This was done following the method proposed by Cox and Snell (1989):

$$R^2 = 1 - \exp\left(\frac{2}{n}(\log L_{\text{null}} - \log L_{\text{full}})\right)$$

Where n is the number of observations in the dataset, $\log L_{null}$ is the log-likelihood of the null model (which excludes all of the fixed effects), and $\log L_{full}$ is the log-likelihood of the full model (which includes all of the fixed effects). $R^2 = 1$ indicates a perfect fit, while $R^2 = 0$ indicates a poor fit. The statistical analysis was performed using the lme4 package in R.

Results and Discussion

DEB model

In this study, we estimated the parameters of a DEB model for yellowfin tuna. Unlike conventional bioenergetic models, the DEB model can describe the dynamic changes in energy budgets across different developmental stages. Using a comprehensive dataset on the growth, maturity, and reproduction of yellowfin tuna throughout their life history, we developed a model that covers the entire life cycle of this species, from an egg to a spawning adult and its eggs.

The parameter estimates for the DEB model are detailed in Table 7 and Table 8. The estimation resulted in an acceptable goodness of fit (GOF = 92.6%), quantitatively showing an overall good match between predictions and observations. In general, the model could correctly capture life-history traits throughout all life stages (Table 4, Figure 3).

Energy budgets for yellowfin tuna are characterized by a dynamic allocation pattern that changes significantly across ontogeny (Figure 4). In the larval stage and early juvenile phase, energy allocation is primarily focused on growth, allowing rapid development during the most vulnerable period of life. A relatively small fraction of the energy is also allocated to maturation, fueling morphological and physiological changes. As internal heating efficiency approaches its maximum, somatic maintenance cost begins to dominate the overall energy budget, resulting in a gradual deceleration of growth. Until the end of the juvenile stage (before puberty), the energy allocated to maturation is used to develop reproductive organs and prepare for the onset of reproduction. After puberty, the fish begins to reproduce, and the energy investment into reproduction increases with size. As the fish approaches its ultimate length, energy allocation is dominated by somatic maintenance (83.6%) and reproduction (15.5%), while a minimal proportion of energy (0.01%) is allocated to growth.

The Tropical Pacific Ocean is characterized by high environmental variability, including phenomena such as ENSO, which affect the distribution and biomass of tunas (Lehodey et al. 1997, 2003, Domokos 2023). Additionally, there are concerns that climate change could alter the magnitude of ENSO, causing higher uncertainty in stock assessment results (Lehodey et al. 2020). Thus, predicting population dynamics while accounting for environmental variability is crucial for the sustainable management of tropical tunas in this region. The Spatial Ecosystem And Population Dynamics Model (SEAPODYM) has been used to predict population dynamics by incorporating environmental forces in the Tropical Pacific Ocean (Lehodey et al. 2003, 2013). Although SEAPODYM is a powerful tool for exploring the mechanisms behind the impacts of environmental changes on tuna migration and population biomass, it cannot capture changes in growth, maturity, and reproduction of fish at an individual level. The DEB model can overcome this issue and provide a foundation for population dynamics models like SEAPODYM. The DEB model is unique in capturing the internal states of fish (energy budget) in relation to external states (environment), enabling the prediction of growth, maturity, and reproduction depending on the experienced environmental conditions. Such an approach could deepen our understanding of how the environment affects tuna movement and biomass, and to better predict population dynamics in response to environmental changes.

Estimating food consumption for archival tagged fish

One of the features of the DEB model is its ability to predict the growth of an individual organism by incorporating environmental factors such as temperature and food abundance. This model thus serves as a valuable tool for estimating field food consumption, which is notoriously difficult to measure at the individual level for free-ranging animals. By using archival tagging data for 28 yellowfin tuna in the WCPO and EPO, where both the length at release and recapture were recorded, we estimated the model's food abundance parameter (f). This parameter was then converted to daily food consumption. As an example, Figure 5 illustrates the application of this method for an archival-tagged fish. The model was fitted to the temperature and growth data to estimate the average f for this fish. The estimated f was then converted to daily food consumption by accounting for the daily changes in temperature and fish size.

On average, the estimated food abundance parameter f for the 28 archival tagged fish was 0.95 (standard deviation: 0.10). The median value for the EPO (0.91, Figure 5) was similar to the assumption made in the model development ($f = 0.93$), suggesting that the model adequately estimated the food availability for the archival tagged fish. The estimated daily food consumption was 281 g on average, ranging from 73 g to 1292 g for fish sized 40-172 cm, which was comparable to the previously reported values for wild fish (284-538 g for fish sized 60-130 cm; Maldeniya (1996), and 0-1105 g for fish sized 48-165.5 cm; Varghese and Somvanshi (2016)).

The estimated daily ration ranged from 1.23% to 5.11% (mean: 2.45%), showing a decreasing trend with increasing size (Figure 6). These estimates were consistent with observations for both wild (1.0-5.5%, Maldeniya (1996)) and captive fish (1.0-10%, Wexler et al. (2003)). The linear mixed-effects model, along with the likelihood ratio tests, revealed that length, temperature, and area significantly affected the daily ration (Table 9 and Table 10). The coefficient of determination for the best model (R^2) was 0.81, suggesting a favorable fit of model predictions to observations. The coefficient of the area effect for the best model (β_1) was -0.275, indicating that the daily ration of fish in the WCPO is reduced by 0.275% compared to those in the EPO under the same size and temperature. In general, the EPO is characterized by higher productivity than the WCPO due to nutrient-rich waters brought by upwelling (Pennington et al. 2006). This can lead to higher prey availability, potentially providing better feeding conditions and supporting greater growth for fish in the EPO. We aim to include more archival tagging data to better capture the trend between the areas.

Our integrated approach using archival tagging and the DEB model reasonably estimated the field food consumption for yellowfin tuna in the WCPO and the EPO. Prey consumption is an important process that determines survival, growth, maturation, and reproduction, and ultimately influences fish movement and population biomass. However, conventional methods to estimate prey consumption for wild fish, such as stomach content analysis, cannot capture the continuous changes in energy intake in response to internal (physiological) and external (environmental) conditions of an individual fish. Our approach addresses this issue and provides a valuable opportunity to explore the mechanisms behind movement and spatial variations in growth that are important in the context of stock assessment.

Note that our DEB model of yellowfin tuna was developed based on the dataset for fish in the EPO. If there are differences in the model parameters that determine the energy allocation pattern between the eastern and western populations, the estimated food abundance could be biased for the fish in the WCPO. Several studies have reported genetic differences between the stocks in the WCPO and the EPO (Sharp 1978, Ward et al. 1997). It is possible, if not likely, that the differences in genetics result in physiological differences between the two populations as a result of fish adapting to their environment. We would like to explore this in the future by developing another DEB model based on the datasets for fish in the WCPO.

Conclusion

We developed a DEB model for yellowfin tuna, covering its entire life cycle. The model favorably captured key life-history traits such as growth, maturity, and reproduction. A key feature of this model is its ability to predict growth as a function of temperature and food abundance. The model can serve as a foundation for developing population dynamics models incorporating environmental forces, allowing stock assessments to be more robust to environmental changes and variation. By using archival tagging data, the model reasonably estimated field food consumption for wild fish. This novel approach enhances our understanding of the foraging ecology of yellowfin tuna and provides insights into the mechanisms behind their movement and spatial growth variations.

References

Bates, D., M. Mächler, B. Bolker, and S. Walker. 2014, June 23. Fitting Linear Mixed-Effects Models using lme4.

Cox, D. R., and E. J. Snell. 1989. Analysis of binary data. Chapman & Hall.

Domokos, R. 2023. Influence of El Niño‐Southern Oscillation on bigeye and yellowfin tuna longline catch per unit effort in the equatorial Pacific. Fisheries Oceanography.

Jusup, M., T. Klanjšček, and H. Matsuda. 2014. Simple measurements reveal the feeding history, the onset of reproduction, and energy conversion efficiencies in captive bluefin tuna. Journal of sea research 94:144–155.

Jusup, M., T. Klanjscek, H. Matsuda, and S. A. L. M. Kooijman. 2011. A full lifecycle bioenergetic model for bluefin tuna. PloS one 6:e21903.

Jusup, M., T. Sousa, T. Domingos, V. Labinac, N. Marn, Z. Wang, and T. Klanjšček. 2017. Physics of metabolic organization. Physics of life reviews 20:1–39.

Kooijman, S. A. L. M., T. Sousa, L. Pecquerie, J. van der Meer, and T. Jager. 2008. From food-dependent statistics to metabolic parameters, a practical guide to the use of dynamic energy budget theory. Biological reviews of the Cambridge Philosophical Society 83:533–552.

Koojiman. 2010. Dynamic energy budget theory for metabolic organisation.

Lehodey, P., M. Bertignac, J. Hampton, A. Lewis, and J. Picaut. 1997. El Niño Southern Oscillation and tuna in the western Pacific. Nature 389:715–718.

Lehodey, P., A. Bertrand, A. J. Hobday, H. Kiyofuji, S. McClatchie, C. E. Menkès, G. Pilling, J. Polovina, and D. Tommasi. 2020, November 4. ENSO Impact on Marine Fisheries and Ecosystems. Wiley.

Lehodey, P., F. Chai, and J. Hampton. 2003. Modelling climate‐related variability of tuna populations from a coupled ocean–biogeochemical‐populations dynamics model. Fisheries Oceanography 12:483–494.

Lehodey, P., I. Senina, B. Calmettes, J. Hampton, and S. Nicol. 2013. Modelling the impact of climate change on Pacific skipjack tuna population and fisheries. Climatic change 119:95–109.

Maldeniya, R. 1996. Food consumption of yellowfin tuna,*Thunnus albacares*, in Sri Lankan waters. Environmental biology of fishes 47:101–107.

Margulies, D., V. P. Scholey, J. B. Wexler, and M. S. Stein. 2016. Chapter 5 - Research on the Reproductive Biology and Early Life History of Yellowfin Tuna *Thunnus albacares* in Panama.

Pages 77–114 *in* D. D. Benetti, G. J. Partridge, and A. Buentello, editors. Advances in Tuna Aquaculture. Academic Press, San Diego.

Pennington, J. T., K. L. Mahoney, V. S. Kuwahara, D. D. Kolber, R. Calienes, and F. P. Chavez. 2006. Primary production in the eastern tropical Pacific: A review. Progress in oceanography 69:285–317.

Sharp, G. D. 1978. Behavioral and Physiological Properties of Tunas and Their Effects on Vulnerability to Fishing Gear. Pages 397–449 *in* G. D. Sharp and A. E. Dizon, editors. The Physiological Ecology of Tunas. Academic Press.

Varghese, S., and V. Somvanshi. 2016. Feeding ecology and consumption rates of yellowfin tuna *Thunnus albacares* (Bonnaterre, 1788) in the eastern Arabian Sea. Indian Journal of Fisheries 63.

Ward, R. O., N. G. Elliott, and B. H. Innes. 1997. Global population structure of yellowfin tuna, *Thunnus albacares*, inferred from allozyme and mitochondrial DNA variation. Oceanographic Literature Review 12:1553.

Wexler, J. B., V. P. Scholey, R. J. Olson, D. Margulies, A. Nakazawa, and J. M. Suter. 2003. Tank culture of yellowfin tuna, *Thunnus albacares*: developing a spawning population for research purposes. Aquaculture 220:327–353.

Table 1. Energy-flow equations.

Description	Equation
Assimilation	$\dot{p}_A = M_1\{\dot{p}_{Am}\}fL^2$
Utilization	$\dot{p}_C = E\left(\frac{M_{\dot{v}}}{L} - 3\frac{d}{dt}\ln L\right) = E\frac{M_1\dot{v}[E_G]L^2 + \dot{p}_S}{\kappa E + [E_G]L^3}$
Somatic maintenance	$\dot{p}_S = \dot{p}_M + \dot{p}_T = [\dot{p}_M]L^3 + M_2\{\dot{p}_T\}L^2$
Growth	$\dot{p}_G = \kappa\dot{p}_C - \dot{p}_S = \kappa\dot{p}_C - \dot{p}_M - \dot{p}_T$
Maturity maintenance	$\dot{p}_J = k_J E_H$
Maturation and reproduction	$\dot{p}_R = (1-\kappa)\dot{p}_C - \dot{p}_J$

Table 2. Equations for state variables.

Description	Equation
Energy in reserve	$\frac{dE}{dt} = \dot{p}_A - \dot{p}_C$
Growth	$\frac{dL}{dt} = \frac{1}{3L^2}\frac{\dot{p}_G}{[E_G]}$
Maturity level	$\frac{dE_H}{dt} = \dot{p}_R\left(E_H < E_H^p\right)$
Reproduction buffer	$E_R = \int \dot{p}_R\left(E_H \geq E_H^p\right)dt$

Table 3. Auxiliary functions

Description	Equation
Shape correction function	$\mathrm{M_1(L, E_H)} = \begin{cases} 1, & (E_H < E_H^b) \\ \frac{L}{L_b}, & (E_H^b \leq E_H < E_H^j) \\ \frac{L_j}{L_b}, & (E_H^j \leq E_H \leq E_H) \end{cases}$
Efficiency of internal heat production	$M_2(E_H) = \begin{cases} 0, & (E_H < E_H^j) \\ \frac{E_H - E_H^j}{E_H^y - E_H^j}, & (E_H^j \leq E_H < E_H^y) \\ 1, & (E_H^y \leq E_H) \end{cases}$
Shape factor	$\delta_M = \frac{\delta_M^1\left(E_H^2 - E_H^b\right) + \delta_M^2\left(E_H - E_H^b\right)}{E_H + E_H^2 - 2E_H^b}, \quad E_H^b \leq E_H < E_H^y$

Table 4. List of zero-variate data used to estimate the DEB model's parameters.

Description	Units	Data	Model	Reference
Egg diameter	mm	0.97	0.924	Margulies et al. 2007
Egg dry weight	ug	42.8	39.83	Margulies et al. 2007
Total length at hatching	mm	25.1	24.77	Margulies et al. 2007
Weight at hatching	ug	30.1	33.28	Margulies et al. 2007
Total length at first feeding	mm	3.32	3.366	Margulies et al. 2007
Weight at first feeding	ug	21.7	23.16	Margulies et al. 2007
Fork length at puberty (FL10)	cm	65	66.17	Schaefer 1998
Ultimate length	cm	179.2	183.9	Wexler et al. 2003
Ultimate weight	kg	169.3	156.8	Wexler et al. 2003

Table 5. List of uni-variate data used to estimate the DEB model's parameters.

Life stage	Data	Source
Embryo	Temperature – Time to hatch	Margulies 2007
	Age – Body mass (dry)	Margulies 2007
Larvae	Age – Standard length	Margulies 2007
Juvenile	Age – Fork length	Wild 1986
	Age – Body mass (wet)	Wild 1986
Adult	Age – Fork length	Wexler 2003
	Length – Body mass (wet)	Wexler 2003
	Body mass – Food conversion ratio	Wexler 2003
	Fork length – Batch fecundity	Schaefer 1998

Table 6. An overview of the archival tagged fish used in this study.

		Release				**Recapture**				
Area	**ID**	**Date**	**Longitude**	**Latitude**	**Length (cm)**	**Date**	**Longitude**	**Latitude**	**Length (cm)**	**Days at liberty**
EPO	L02783	2022/5/3	249.95	5.00	42	2023/4/20	262.35	15.10	92.5	352
EPO	L02793	2022/5/3	249.95	5.00	45	2022/9/21	261.58	0.40	57.1	141
EPO	L02719	2022/5/3	249.94	5.00	48	2022/9/17	265.42	3.53	55.8	137
EPO	L02659	2022/5/3	249.95	5.00	46	2022/8/6	261.75	4.28	52	95
EPO	L02786	2022/5/3	249.95	5.00	40	2022/7/29	260.75	4.47	48.5	87

EPO	L02628	2022/5/3	249.95	5.00	45	2022/6/4	249.12	4.60	48.5	32
EPO	2190190	2022/4/16	264.47	0.11	60	2022/5/27	261.33	1.27	63	41
EPO	L02785	2022/4/11	264.47	0.09	47	2022/7/11	266.17	-0.05	53	91
EPO	2190192	2022/4/11	264.47	0.09	69	2022/6/5	264.28	2.70	72.5	55
EPO	2190213	2022/4/5	264.45	0.07	74	2022/7/6	263.68	2.50	78.5	92
EPO	L01441	2019/4/28	249.93	4.97	48	2019/8/19	256.10	5.80	59	113
EPO	1890108	2019/4/15	264.40	0.18	64	2019/6/20	256.22	0.27	73	66
EPO	B1180	2013/3/7	250.83	10.32	135	2013/9/17	250.83	10.32	172	194
EPO	B1156	2013/3/5	250.83	10.32	104	2013/9/17	250.83	10.32	125	196
EPO	B1204	2013/3/4	250.83	10.32	88	2013/9/20	251.07	10.28	100	200
EPO	D4387	2009/9/15	279.87	7.32	67	2010/5/27	280.93	6.37	92	254
EPO	D0764	2007/1/30	279.87	7.32	58	2009/4/21	274.97	5.53	127	812
EPO	C0209	2006/4/6	264.80	2.22	52	2006/8/21	240.15	6.00	71	137
EPO	L02795	2022/4/11	264.47	0.09	47	2022/7/15	251.12	4.47	58	95
EPO	A0121	2009/10/24	219.83	-2.03	79	2010/2/2	219.92	-1.67	94	101
WCPO	340038	2012/1/29	150.81	-6.28	63	2012/3/27	153.93	-2.29	64	58
WCPO	450248	2018/8/14	-178.83	-4.68	93	2018/12/1	175.53	-4.94	115	109
WCPO	339748	2012/1/27	152.39	-4.98	55	2013/11/17	152.95	-6.02	94	660
WCPO	340037	2012/1/29	150.81	-6.28	66	2013/1/17	152.24	-5.71	115	354
WCPO	381004	2013/4/19	150.83	-6.52	72	2013/11/1	152.95	-7.53	93	196
WCPO	340034	2012/1/29	150.81	-6.28	64	2012/12/16	149.51	-3.17	94	322
WCPO	9846	2006/9/24	146.44	-4.34	98	2007/1/26	150.53	-7.77	117	124
WCPO	270133	2010/6/5	-162.19	5.88	79	2011/4/3	-161.00	4.50	98	302
WCPO	481510	2021/8/4	-166.11	2.19	57	2021/9/7	176.95	4.03	61	34
WCPO	270134	2010/6/5	-162.19	5.88	98	2011/10/6	-166.55	5.88	119	488
WCPO	382162	2013/4/20	150.79	-6.53	72	2013/8/30	149.18	-3.66	85	132
WCPO	281014	2011/4/25	150.65	-6.67	51	2012/3/10	146.32	-3.91	94	320

WCPO	340030	2012/1/29	150.81	-6.28	64	2012/12/24	151.13	-4.40	71	330
WCPO	382297	2013/4/20	150.93	-6.69	71	2013/12/22	175.81	-8.60	106	246

Table 7. List of standard DEB parameters for yellowfin tuna.

Description	**Symbol**	**Unit**	**Value**
Maximum assimilation rate	$\{\dot{p}_{AM}\}$	J·cm^{-2}·d^{-1}	82.56
Cost of structure	$[E_G]$	J·cm^{-3}	7845
Energy conductance	$\dot{v}$	cm·d^{-1}	0.06794
Somatic maintenance rate	$[\dot{p}_M]$	J·cm^{-3}·d^{-1}	12.72
Somatic maintenance rate	$\{\dot{p}_T\}$	J·cm^{-2}·d^{-1}	1743
Maturity maintenance rate coeffcient	k_J	d^{-1}	0.002
Reserve allocation to soma	κ	–	0.8372
Maturity at birth	E_H^b	J	0.1329
Maturity at puberty	E_H^p	J	3.246·10^7

Table 8. List of auxiliary parameters specific to the tuna DEB model.

Description	**Symbol**	**Unit**	**Value**
Maximum reserve energy density	$[E_M]$	J·cm^{-3}	1.2153e·10^3
Maturity at hatching	E_H^h	J	0.04996
Maturity at metamorphosis	E_H^j	J	7107
Half-saturation maturity	E_H^2	J	1.314
Maturity at thermogenesis	E_H^y	J	1.778·10^5
Arrhenius temperature	T_A	K	6407
Shape factor in the larval stage	δ_M^1	–	0.1314
Shape factor in the adult stage	δ_M^2	–	0.2737
Avg. no. of spawned batches	N	–	51

Table 9. Results of likelihood-ratio model comparisons of the linear mixed-effects model of daily ration. The Chi-squared statistic (Chisq) and p-value were calculated from the likelihood ratio and used to assess the significance of the fixed effects on daily ration.

Model	**AIC**	**log-likelihood**	**deviance**	**Chisq**	**df**	***p*-value**
ID	177.9	-85.96	171.9			
Length + ID	94.21	-43.10	86.21	85.71	1	< 0.01
Length + Temp + ID	45.79	-17.89	35.79	50.41	1	< 0.01
Length + Temp + Area + ID	43.68	-15.84	31.68	4.11	1	0.042

Table 10. Summary table of the best linear mixed-effects model of daily ration. Parameter estimates for the fixed and random effects are represented with their standard errors (SE), standard deviations (SD), and t-values.

Fixed Effects	**Estimate**	**SE**	**t-value**
Intercept (β_0)	-1.307	0.710	-1.840
AreaWCPO (β_1)	-0.275	0.123	-2.221
Length (β_2)	-0.026	0.002	-14.01
Temperature (β_3)	0.229	0.027	8.796
Random Effects	**Variance (σ^2)**	**SD**	
ID	0.087	0.295	

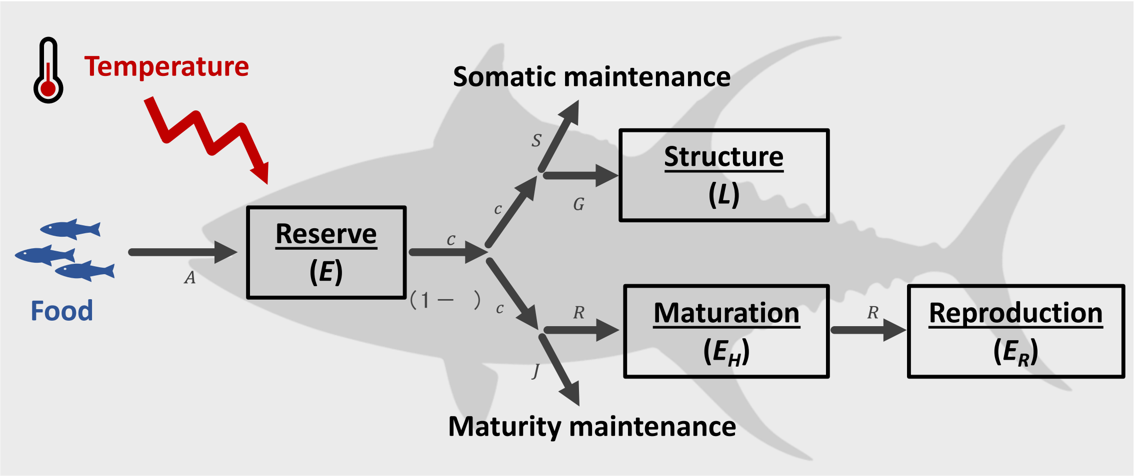

Figure 1. Schematic representation of the DEB model.

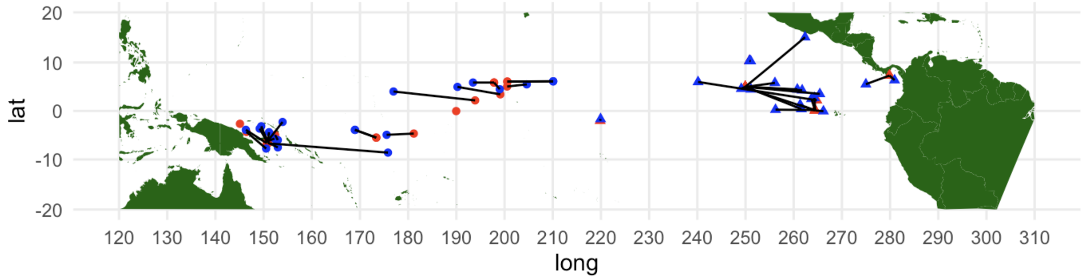

Figure 2. Positions at release (red) and recapture (blue) for the archival tagged fish used in this study.

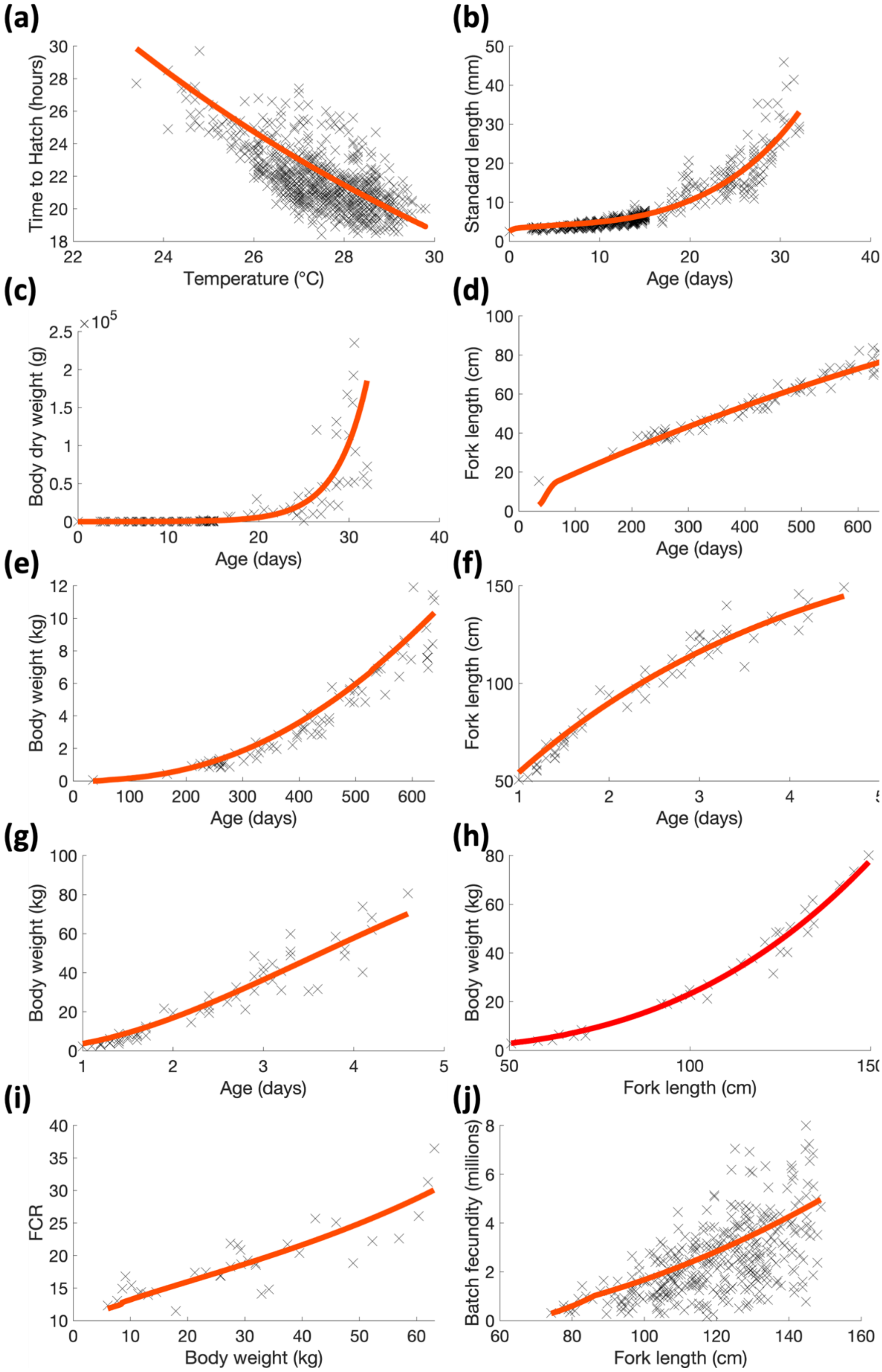

Figure 3. Comparison of observational data (x) and the model predictions (red line).

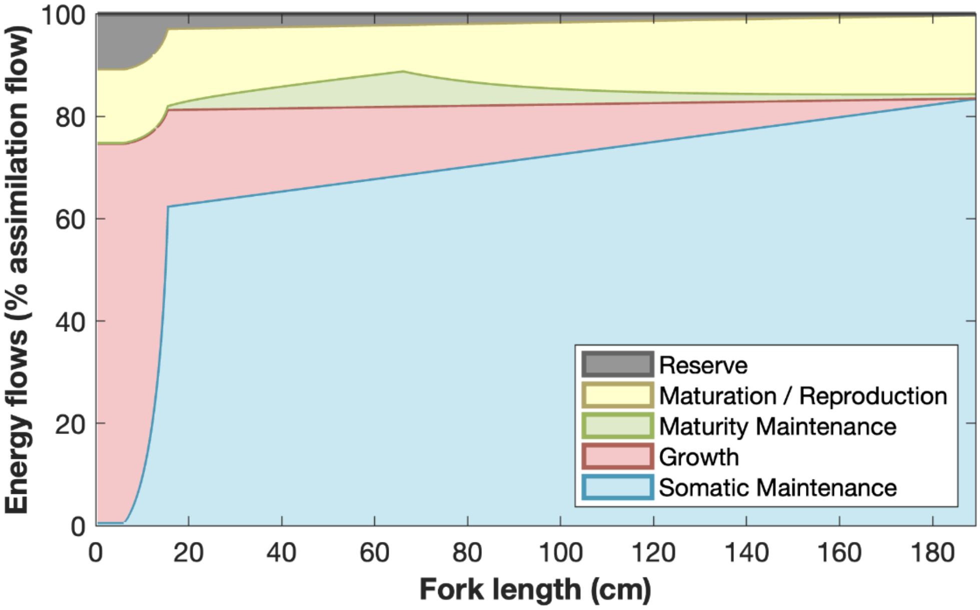

Figure 4. Energy budget of yellowfin tuna. The dark gray area on top represents the reserve dynamics (difference between the assimilation flow and utilization flow). The utilization flow is divided between the maturation/reproduction flow (yellow), the maturity maintenance flow (green), the growth flow (red), and the somatic maintenance flow (blue).

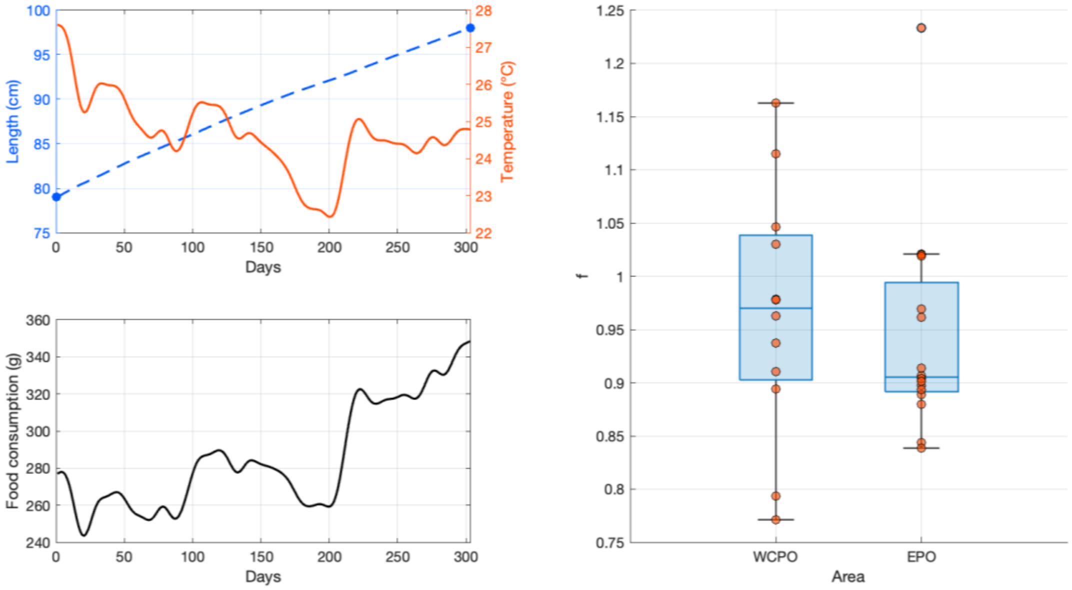

Figure 5. Estimating field food consumption using the DEB model for yellowfin tuna. The DEB model was forced with the recorded daily ambient temperature (red curve in the top left panel) and food abundance (free parameter) that best fits the length at release and recapture (blue dots

on the top left panel) of an archival-tagged fish (ID = 270133). This was used to estimate the scaled food abundance (*f* = 0.92) and the growth trajectory (blue dashed curve in the top left panel). The estimated food abundance was then converted to daily food consumption (black curve in the bottom left panel). The estimated food abundance was also compared between the areas (right panel). The red dots denote the values for individual fish.

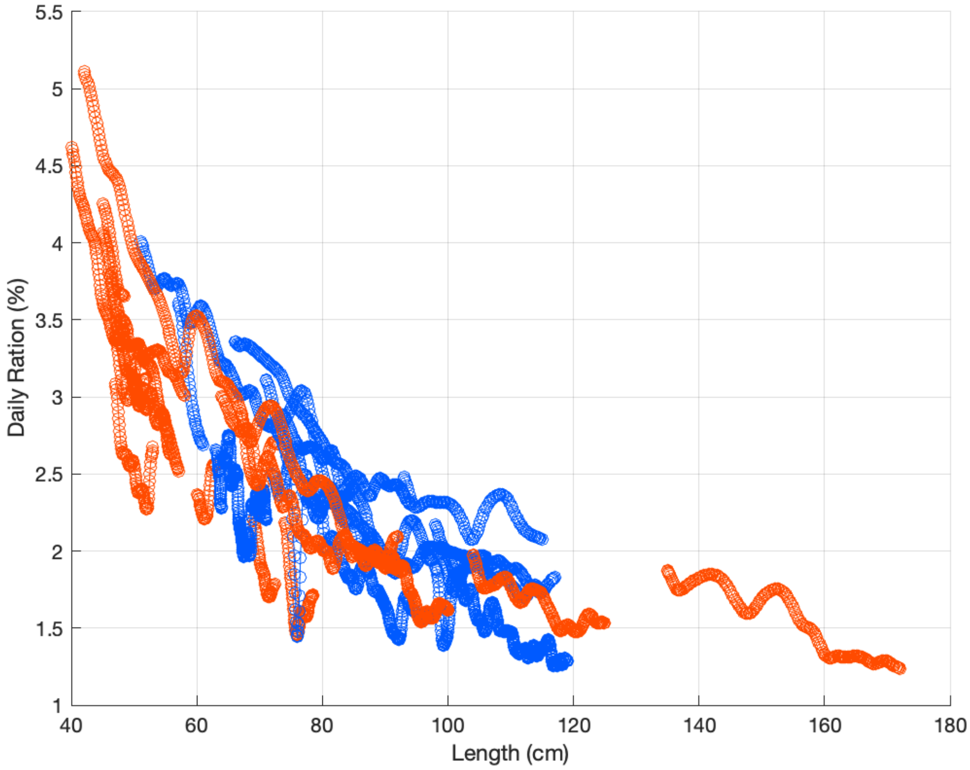

Figure 6. Daily ration as a function of length in the WCPO (blue) and the EPO (red).